Mandrel-Based Fiber Optic Sensors for Acoustic Detection of Partial Discharges – a proof of concept

Sanderson E. U. Lima, *Student Member*, Orlando Frazão, Rubem G. Farias, Francisco M. Araújo, Luís A. Ferreira, José L. Santos and Vladimiro Miranda, *Fellow IEEE*

***Abstract* — Acoustic emission monitoring is often used in the diagnosis of electrical and mechanical incipient faults in high voltage apparatus. Partial discharges are a source of failure in power transformers and the differentiation from other sources of acoustic emissions is of the utmost importance. This paper reports the development of a new sensor concept - mandrel-based fiber optic sensors - for the detection of incipient faults in oil-filled power transformers, taking direct measurements inside a transformer. These sensors can be placed in the inner surface of the transformer tank wall, not affecting the insulation integrity of the structure, and improving fault detection and location. The applicability of these acoustic sensors in air, water and oil is investigated and the paper presents the promising results obtained, which will allow the industrial development of practical solutions.**

***Index Terms*— Power Transformer Insulation, Partial Discharges, Optical Fiber Sensors, Acoustic Emission, Fabry-Perot Interferometer.**

I. Introduction

ACOUSTIC emissions (AE) in power transformers are generated by electrical sources (such as partial discharge and arcing) and by mechanical sources (such as loose clamping, bolts, or insulation parts). It is possible to identify the AE source using the characteristic signature of each emission; indeed, from this signature emission parameters such as burst rate and count rate can be evaluated and compared with those derived from known AE sources [1]-[3].

Insulation degradation is mainly associated with the occurrence of partial discharges (PDs). These are an electrical phenomenon that occurs within a transformer whenever the voltage stress is sufficient to produce ionization in voids or inclusions within a solid dielectric, at conductor/dielectric interfaces or in bubbles within liquid dielectrics such as oil. High-frequency transient current discharges appear repeatedly and will progressively deteriorate the insulation, ultimately leading to breakdown [4]. In power transformers, the levels of PDs are an indicator of the insulation condition, because they result of localized electrical breakdown that should not be present in significant values in a good insulation system. Any PD activity has detrimental effects on the insulating materials (paper, polymers, etc) surrounding the conductors and degrades the insulating properties of the oil, and thus its prognosis and diagnosis are of utmost importance [5].

Acoustic sensing has been one of the first successful applications of fiber optic sensors [6]-[8] and the literature on optical fiber interferometry for acoustic and ultrasonic sensing is extensive [9]. Underwater acoustic sensing has been studied since the end of the 1970s and many configurations were proposed to optimize system performance [10]-[12]. This application is well suited for interferometric sensors because the sensitivity of such sensors is high and scalable by selection of the sensing fiber length. The operation of these sensors is based on the optical fiber path length modulation due to the acoustic wave pressure. High-performance interferometric demodulation techniques enable phase resolutions as small as 10^{-6} rad [13]. Furthermore, acoustic sensing does not require dc sensitivity, which is the domain where interferometric sensors are not attractive because of their inherent susceptibility to signal drift (in the limit, imposed by temperature fluctuations). Michelson, Mach-Zehnder and Sagnac interferometric configurations were used in successful designs of acoustic sensors [14]-[16]. However, a common problem with these sensors is the requirement for long sensing lengths to achieve sufficient acoustic sensitivity.

Acoustic detection with fiber Bragg grating (FBG) based sensors is possible if an acoustic wave is able to transfer energy to a fiber (inducing a strain along the axes), producing, therefore, a shift of the Bragg wavelength. Considering the high stiffness of the fiber material, such acoustically induced wavelength shifts are small, demanding a high-resolution interrogation system [13]. In 1996 the first work with FBGs for sensing of ultrasonic pressure fields was reported [17]. One of the most important results of this pioneer work was the understanding that the frequency of the incident wave has an upper limit to be correctly detected with FBGs, i.e., the grating length should be less than half the ultrasonic field wavelength in the fiber core. Another significant development in underwater acoustic sensing using FBGs relied on the utilization of a homodyne detection method, resulting in a linear relationship between the incident wave pressure and the output signal [18]. Other works dealt with several issues related with acoustic sensing using FBGs [19]-[23].

With the intrinsic advantages of fiber optics sensors in

Manuscript received May 25, 2009. S.E.U Lima acknowledges the support of Fundação para a Ciência e a Tecnologia – FCT (PhD fellowship SFRH/BD/48724/2008).

The authors are all with INESC Porto, Instituto de Engenharia de Sistemas e Computadores do Porto, Portugal.

S.E.U. Lima, O. Frazão and J.L. Santos are also with FCUP – Faculty of Sciencies of the University of Porto, Portugal (e-mails: sanderson.lima@fc.up.pt, ofrazao@inescporto.pt; jlsantos@inescporto.pt).

R.G. Farias is also with Faculty of Computer Engineering of UFPA, the Federal University of Pará, Brazil (email: rgfarias@ufpa.br).

V. Miranda is also with FEUP – Faculty of Engineering of the University of Porto, Portugal (email: vmiranda@inescporto.pt).

mind, this paper describes the development of new fiber sensors for the detection of acoustic emissions with characteristics adapted to utilization in power transformers. A conventional Michelson interferometer and other two optical sensing elements, based on FBGs and Fabry-Pérot Cavities (FPCs), were attached to an air-backed mandrel for acoustic amplification. A laser was used to interrogate the sensors and the detection scheme used a computer-based feedback loop, in a homodyne configuration, to tune the laser wavelength emission and track the quadrature point, optimizing the readout sensitivity. The sensitivity obtained with the different sensing head configurations is compared and some ways of system performance improvement are discussed. Additionally, the effects in the characteristics of the sensing heads when immersed in different fluids (water and oil) are addressed.

The paper primary intent is to demonstrate a *proof of concept*: that the optical sensing concepts described can be applied to acoustic detection of partial discharges. The experimental tests describe the uses of acoustic transducers under a concept that better suits such primary purpose. In order to have a convincing demonstration, one did not resort to the use of "artificial" PD sources (e.g. rod-plates electrodes), because they can't reproduce accurately the real characteristics of PDs (energy intensity, number of charges, pulse number, pulse length of time, frequency content, spark signature, strikes rate, etc) in power transformers.

Instead, data have been collected from literature (front wave pressure, duration, frequency content, repetition rate, etc), which allowed the reproduction of acoustic waves that are generated by partial discharges. This procedure, from the acoustic point of view, can reproduce with high fidelity the acoustic characteristics of a PD occurrence.

Certainly, a new research phase is now envisaged – it will correspond to the transformation of prototype into product, but it is out of the scope of this paper. Issues to be researched involve the difficulty in simulating the complex environment of the inner part of a real power transformer (dimensions, materials, insulation degradation, insulation voids, hot spots, etc). There are a number of issues that only can be characterized in real on-site tests (in a power plant) and with an engineering product design of the final detector product – namely, to address concerns such as influence in the electromagnetic field which, form a theoretical point of view, seem negligible but however must be confirmed or minimized in a practical industrial design, in a future research effort.

II. Detection and Location of Acoustic Emission of Partial Discharges in Power Transformers

The energy released in PDs produces a number of effects, resulting in chemical and structural changes and electromagnetic emissions [24]. PDs are pulse-like in nature and its acoustic detection is based on the mechanical pressure wave emitted from the discharge. These waves propagate within the transformer, throughout the surrounding oil and hit the transformer tank wall.

In general, it is important not only to detect PD activity but also to give an indication of the PD source location. Traditional methods use piezoelectric sensors mounted on the outside of the wall of the transformer tank to achieve acoustic PD detection. This method has problems with the high attenuation in the wall, as well as the issue of multiple routes between source and sensor that can diminish dramatically the accuracy of PD location [25]. Furthermore, the energy content of a PD is small, and can leave to no observable evidence on the surrounding insulating structure.

The accuracy of the acoustic PD location approach depends upon being able to detect the PD pressure wave, and to separate the resulting signals from background noise. Thus, a high sensitivity sensor system is needed to detect the acoustic waves in different points of the transformer and a robust signal processing system is required to correct interpretation of the results to perform a meaningful PD source location [1-3]. These problems can be avoided using optical fiber sensors that can be placed inside the transformer tank without affecting the insulation integrity. This intrusive configuration is particularly useful in substations environments where there is a high level of outside interference. In addition, the accuracy of the source location can be very improved using intrusive sensors because it is possible identify the direct path signals that reach each sensor [25]-[28].

The first successful application of optical fiber sensors to PD detection was reported in 1996 by Zargari and Blackburn [26]. They developed an intrinsic fiber sensor based on a Michelson interferometric configuration where the interaction section is formed by coiling 110 m of momonode fiber into a doughnut shape. In 1998, the same authors worked out another non-intrusive fiber optic sensor for PD detection that is mounted externally on brushing of a current transformer [27]. In a similar approach, Zhao demonstrated an acoustic sensor based on a Mach-Zehnder interferometer incorporating in one of its arms an optical fiber coil [28]. The sensor response to plane waves was investigated for various angles of incidence and frequencies in the range of interest (50 to 300 kHz). The sensor responded reasonably flat and enabled the locating of the PD source by triangulation. Other optical sensing configurations to PD acoustic detection, e.g. using diaphragm-based extrinsic FPCs, can be found elsewhere [29]-[31].

The acoustic emission of PDs has wideband frequency content (10 to 500 kHz). In gases, the high frequencies are very attenuated, leaving only vibrations in the audible sound range. In liquids and in some solids, the attenuation of high frequencies is not so severe, and the acoustic wave from PDs will have the ultrasonic components as well as audible components. For detecting the presence of such ultrasonic components, considering the attenuation and the energy density, a sensor with response in the frequency range of 20 to 100 kHz is considered a good acoustic PD detector [32]. Figure 1 shows the wave shape of a real PD acoustic signal (left) in time domain and (right) his frequency content.

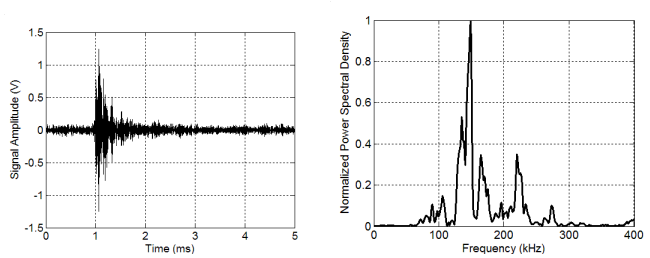

Fig. 1. Acoustic emission impulse detected by a piezoelectric sensor closed to a real PD source: (left) time domain signal and (right) his frequency content.

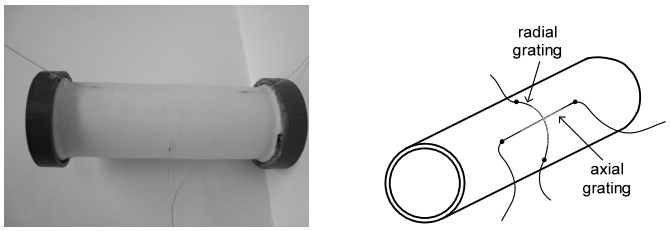

Fig. 2. Sensing head using a mandrel and two fiber Bragg gratings.

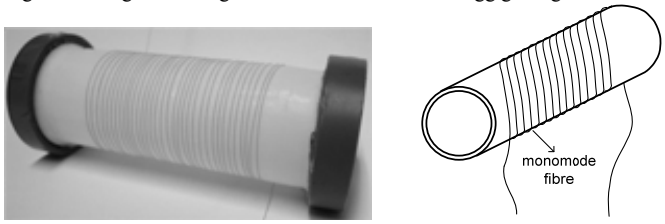

Fig. 3. Sensing head using a Michelson interferometer.

III. Sensing Heads

A. Fiber Bragg Gratings

This sensing head is shown in Figure 2. It consists of two FBGs attached to the wall of a compliant mandrel that is used as before as a passive acoustic amplifier. The operation of the sensor is based on the Bragg wavelength shift induced by the strain that the mandrel transfers to the fiber when an acoustic pressure wave strikes the cylinder wall. The project of the compliant cylinder is done selecting the dimensional parameters (radius, length and thickness) and the characteristics of the material (Young modulus and Poisson ratio) that maximizes the sensor sensitivity and satisfies some requirements (e.g. maximum static pressure operation, directionality and frequency response).

A theoretical evaluation was done using the mathematical model for a thin walled cylinder to obtain the displacements values in the axial and radial directions in terms of *n* (the nodes of circumferential waves) and *m* (the number of axial half-periods). From such model, the resonances frequencies are given by [33], [34]:

$$\omega_{m,n}^2 = \frac{E}{\rho(1-\upsilon^2)R^2}\left(\frac{(1-\upsilon^2)\lambda^4 + a^2(\lambda^2+n^2)^4}{n^2+(\lambda^2+n^2)^2}\right) \quad (1)$$

where E is the Young Modulus, υ is the Poisson ratio, ρ is the material density, R, L and t are, respectively, the radius, length and thickness of the cylinder, $\lambda = m\pi R / L$ and

$$a^2 = \frac{t^2}{12R^2} \quad (2)$$

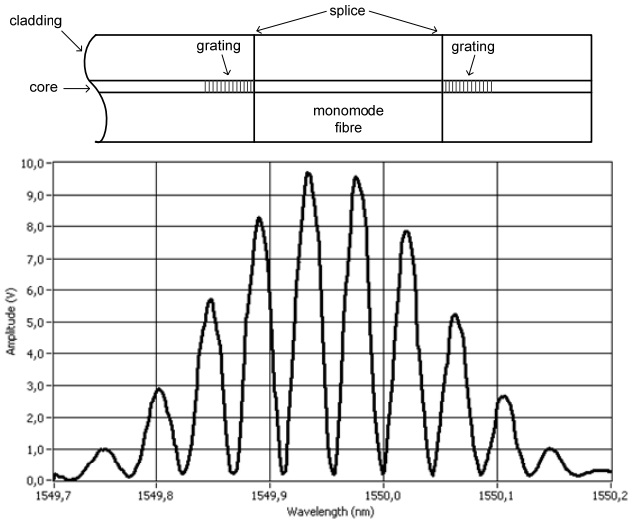

Fig. 4. Fabry-Perot cavity and its interferometric channeled spectrum.

For the present application, it is relevant to determine the values of m and n for which the smallest natural frequency, of predominantly transverse vibration, occurs. This condition is obtained for $m=1$ and n is a nearest integer from n' [33]:

$$n' = \sqrt{\lambda\left(\sqrt[4]{\frac{(1-\upsilon^2)}{a^2}} - \lambda\right)} \quad (3)$$

Another important normal mode, which affects more directly the response of the fiber attached circumferentially, is the "breathing" mode with $n=0$ and $m=1$. The fundamental modal frequency resonance ($\omega_{1,0}$) associated with this pure radial motion that corresponds to extensional vibrations is

$$\omega_{1,0}^2 = \frac{E}{\rho(1-\upsilon^2)R^2}\left[(1-\upsilon^2) + \frac{t^2\pi^4R^2}{12L^4}\right] \quad (4)$$

If the mandrel is immersed in a fluid, in general the resonance frequency will lower due to the added mass effect and it will also decrease the amplitude at the peak due to re-radiation of acoustic energy. The response is expressed as the normalized radial displacement, $W_{1,0}(\omega)/R$, produced by a pressure wave Δp_ω of frequency ω [35]:

$$\frac{W_{1,0}(\omega)}{R} = \Delta p_\omega \frac{R(1-\upsilon^2)}{Et} \frac{1}{\left(\frac{\rho_0(1-\upsilon^2)R^2\omega^2}{E}\right)} \cdot \frac{1}{\left(1+\frac{\rho_0}{\rho_1}\frac{K_0(\gamma R)}{\gamma K_1(\gamma R)}\right) - 1 - \frac{t^2\pi^4R^2}{12L}} \quad (5)$$

where ρ_0, ρ_ℓ are the air and fluid densities, $K_0(\gamma R)$, $K_1(\gamma R)$ are the modified Bessel functions of order zero and one, and

$$\gamma^2 = \frac{\pi^2}{L^2} - \frac{\omega^2}{v_l^2} \quad (6)$$

The parameter v_l is the sound velocity into the fluid. The parameter γ is imaginary for frequency f above $v_l/2L$, indicating that the cylinder is reinforcing the sound wave [35].

The sensor is designed to monitor acoustic emissions inside a transformer. Thus, the materials to be used for its fabrication must be dielectric to avoid problems with the insulation system. Also, a relatively flat frequency response in the range 10-50 kHz is desirable. In view of these requirements and using the above equations, the mandrel was designed as a cylinder of polycarbonate plastic tube (teflon), 30 mm long, with an outer diameter of 12 mm and a thickness of 0.5 mm.

B. Michelson Interferometer

A conventional fiber Michelson interferometer is used as a comparative basis for the other sensing heads. This interferometic configuration has been successfully used as hydrophones and acoustic sensors [6]-[12]. The acoustic wave induces a shift of the relative phase of the optical fields in the sensing and reference arms. Here, this basic sensing structure is integrated with a passive acoustic amplifier (mandrel) and a high resolution detection system is used to translate the optical phase information into an electrical signal suitable for further processing.

The interferometer sensing arm is coupled to an air-backed mandrel made of a polycarbonate plastic tube. A length of 120 cm of a normal single-mode fiber (SMF28 - 9/125/250 μm) was wound around it. The reference arm has the same length and was wound around a cylinder to make the bending losses similar in both arms. Figure 3 shows a photograph of the air-backed mandrel and a schematic of the sensing head.

C. Fabry-Pérot Interferometer

The third sensing head developed was a fiber Fabry-Pérot Interferometer (FPI) with two identical FBGs that operate as the cavity mirrors. The sensing head fabrication process starts by cutting a 50% reflectivity FBG at the middle to produce two identical half-length Bragg gratings. Then, a piece of monomode fiber is spliced between the Bragg gratings to produce the FPC. Finally, the two ends of the FPC are bonded to the compliant mandrel in a manner similar to that used in the FBG sensing head configuration. Figure 4 shows the FPI using two FBGs and its interferometric channeled spectrum. This pattern is characterized by a superposition of a slowly varying envelope associated with the FBG reflection spectrum and an interference fringe pattern relative to the FPI.

The sensor operation is based on the transduction of the cylinder vibration, in the presence of an acoustic wave, into a fiber longitudinal strain. This dynamic pressure induces changes in the grating spectrum (Bragg wavelength shift) and in the interference fringe pattern (cavity length variation). Since the two identical Bragg gratings are submitted simultaneously to the same strain, a shift of the spectrum pattern is obtained without deformation. The dynamic strain signal also induces a variation of the cavity length that modulates the round-trip propagation phase shift in the FPI. The implemented interrogation system detects the optical power modulation induced by the relative shift of the central fringe (fringe with maximum amplitude) with respect to the laser wavelength. Considering that the FBG spectral envelope and the interferometric fringes move synchronously under the action of the acoustic wave, there is no modulation of the central fringe associated with the spectral displacement of the envelope.

D. Sensor Interrogation

The detection approach used to interrogate all sensing heads is shown in Figure 5. The optical interrogation system is based on a tunable laser and a feedback loop receives the photodetector output signal through an acquisition board and controls the wavelength of the laser emission to compensate the low-frequency variations of the photodetector signal (drift information) induced by a quasi-static parameters (e.g. temperature changes).

Therefore, the detection of acoustic waves, which are at much higher frequency range, is not effect directly by temperature changes. Thus, the high frequency signal is recovered directly from the photodetector output (low-bandwidth operation). However, temperature changes can affect the readout sensitivity because the interferometer drift along its transfer function when temperature changes.

This issue was overcome implementing a computer-based active homodyne detection system that maintains the interferometer locked at its quadrature condition, which is the position of highest phase sensitivity. Due to the interferometric operation of the sensing heads, the most important non-linearity present is associated with the co-sinusoidal interferometric transfer function.

However, the interrogation approach implemented keeps the interferometers always locked at the quadrature condition, which is also the position of highest linearity. Thus, the detection scheme maintains the system operating in the quasi-linear region of the interference fringe spectrum.

This operation condition results in a linear relationship between the incident wave pressure and the output signal of the detection scheme and, consequently, the complexity of the processing system to extract information of the measured signals is reduced if compared with other detection schemes. LabVIEW® software was used to perform the control process and to analyze signals.

IV. RESULTS

In the experimental setup, a piezoelectric transducer (PZT) 200LM450-ProWave was used as an acoustic source to simulate the pressure wave from a partial discharge. In underwater applications, the PZT has a transmitting sound pressure level of 155 dB (@ 0 dB ref 1μPa/Vrms) with a center frequency of 200 kHz. The sensor signal is collected by a data acquisition (DAQ) board and further processing is done using the LabVIEW® software.

A. Michelson Interferometer Sensing Head

The performance of the sensing head based on the

Michelson interferometer was investigated and the results were also used to verify the correct operation of the detection system and to establish a reference for the other sensing configurations studied in this work. In a first experiment, the operation of the detection scheme was tested with temperature variations on the sensing arm. The results show that the feedback loop (computer-based) can control the laser emission wavelength to compensate the temperature variations and maintain the interferometer locked at a quadrature point.

The stored data is a fast Fourier transform (FFT) of the time domain photodetector electrical signal. Figure 6 (up) shows the FFT spectrum of the sensor output signal when the PZT is used to produce a 10 kHz acoustic wave in an underwater test (the PZT was 10 cm away from the sensing head). As can be observed, the signal is 50 dB above the noise floor. Tests were done to evaluate the sensor response in function of frequency and distance. Figure 6 (down) shows the attenuation of the sensor signal as a function of the distance between the acoustic source and the sensor at frequencies of 3, 10 and 30 kHz.

These results show the frequency influence in the sensor response: for low frequencies and short distances, the sensor signal is stronger and the distance attenuation is more accentuated.

The demodulation system has a noise floor of $V_{RMS\text{-}noise}$= 0.3 mV, and the PZT has a sound emitted pressure level of 105 Pa at 10 kHz. Thus, at a distance of 10 cm (the standard distance for characterization of the acoustic emitter), an acoustic receiving sensitivity of -235 dB (@ 0 dB = 1 Vrms/µPa) was obtained, which allows a pressure resolution level of 170 Pa at 10 kHz.

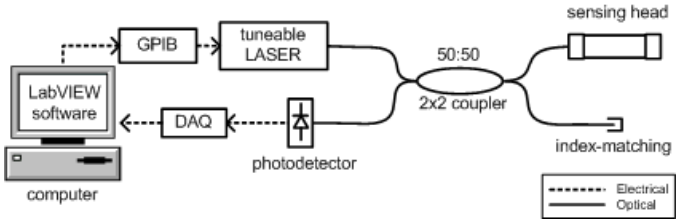

Fig. 5. Sensor system setup comprising a homodyne signal detection scheme with active computer-based phase tracking.

B. FBG Sensing Head

In this sensing configuration the sensor signal is proportional to the Bragg wavelength shift relative to the laser line (at the start up the laser line was tuned to the inflection point of one of the lateral edges of the FBG spectral reflectivity function).

The results obtained when the FBG is attached to the mandrel in radial or axial layouts are distinct, the best performance being associated with the radial configuration.

Figure 7 shows the FFT spectrum of the output signal relative to the radial FBG configuration when an acoustic wave of 10 kHz was produced by the PZT in an underwater test, again 10 cm away from the sensing head. As it can be seen, the signal level is -20 dB and the noise level is -70 dB.

Figure 8 shows the attenuation of the sensor signal as a function of the distance between the acoustic source and the sensor at frequencies of 3, 10 and 30 kHz for the axial (up) and radial (down) configurations.

The sensitivity test was performed at the same conditions of the previous one (at 10 kHz, 10 cm away and $V_{RMS\text{-}noise}$= 0.3 mV). An acoustic receiving sensitivity of -240 dB and a pressure resolution level of 320 Pa are obtained.

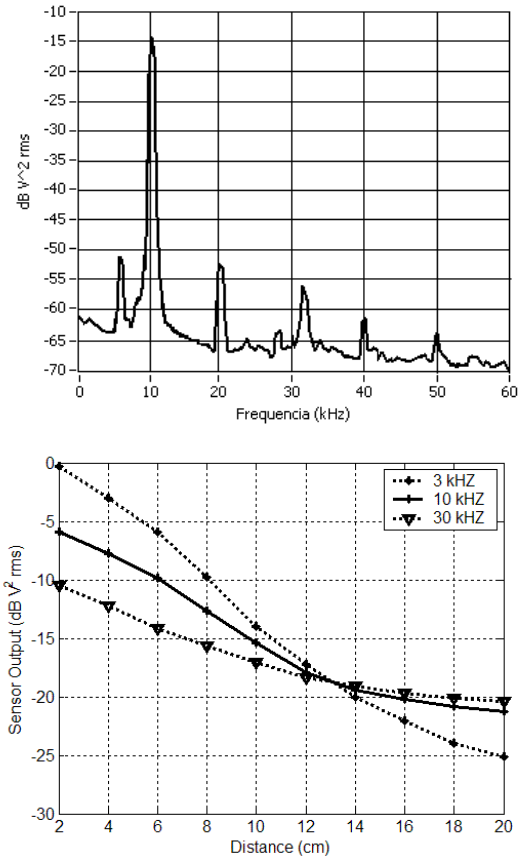

Fig. 6. (up) FFT of the signal output of the sensor based on the Michelson interferometer when the PZT is used to produce an acoustic wave in water at a frequency of 10 kHz (10 cm distance). (down) Distance signal attenuation at frequencies of 3, 10 and 30 kHz.

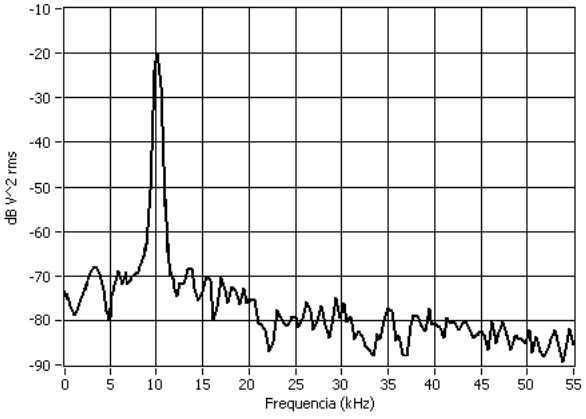

Fig. 7. FFT of the signal output of the sensor based on a single FBG when the PZT is used to produce an acoustic wave in water at frequency of 10 kHz (10 cm distance).

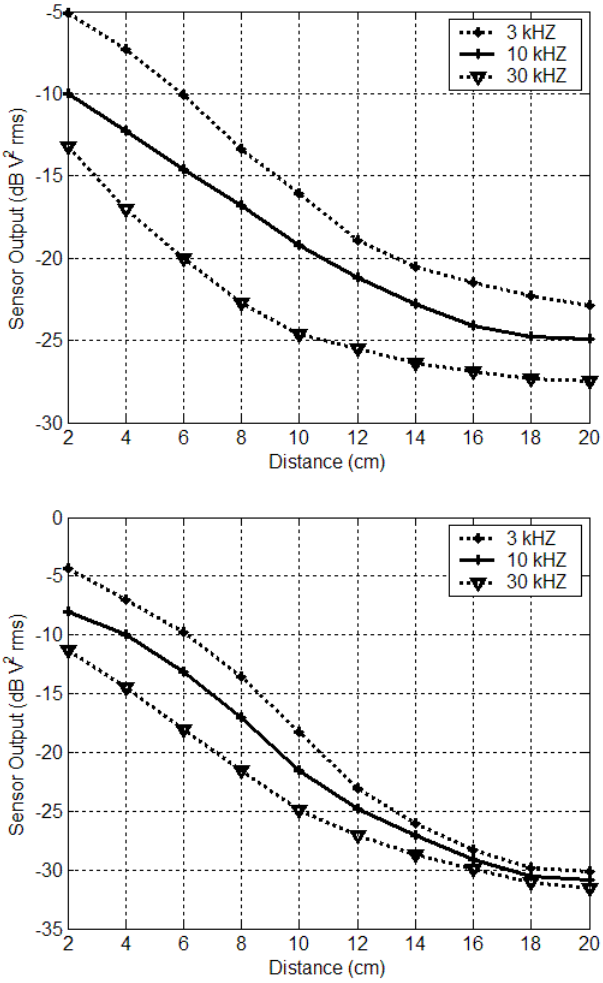

Fig. 8. Distance signal attenuation for the FBG sensor at frequencies of 3, 10 and 30 kHz for the axial (up) and radial (down) configurations.

C. *Fabry-Pérot Interferometer Sensing Head*

The sensing structure based on the described FPI was developed and tested in order to improve the sensor pressure resolution at the operational frequency range (10 to 50 kHz). A FBG-based cavity with a length of 30 mm was illuminated with broadband radiation around 1550 nm, resulting in a channeled spectrum with a periodicity of ≈ 30 pm within the gratings spectral bandwidth (Figure 4). The laser line is tuned to a quadrature position of the central fringe at the start-up. Figure 9 (up) shows the FFT spectrum output signal of the FPI sensor when, in an underwater test, a 10 kHz acoustic wave was produced by the PZT in the same conditions as before (sensing head 10 cm away from the emitter). As it can be observed, the signal level is -13 dB and the noise level is -70 dB, resulting into a signal-to-noise ratio of 57 dB. Figure 9 (down) gives the attenuation of the sensor signal in function of the distance between the acoustic source and the sensor at frequencies of 3, 10 and 30 kHz.

This sensor configuration enables a higher receiving sensitivity of - 233 dB that results in a pressure resolution level of 140 Pa at the frequency of 10 kHz. This means that, compared with the sensing head based on a single FBG, this interferometric approach doubles the resolution level.

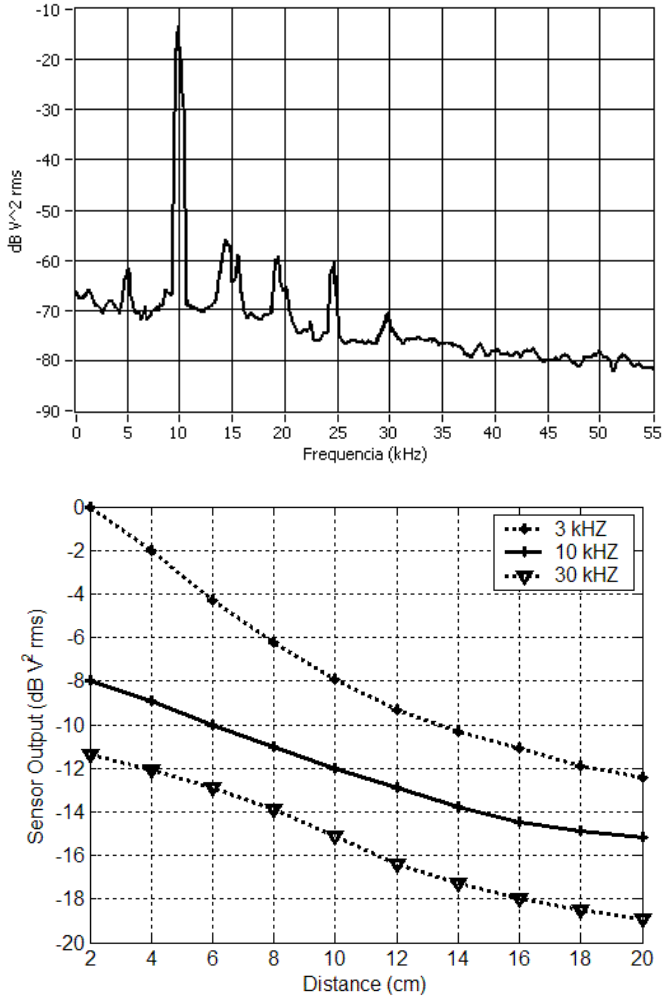

Fig. 9. (up) FFT of the signal output for the sensor based on the FPI configuration when the PZT is used to produce an acoustic wave at a frequency of 10 kHz in water (10 cm distance); (down) distance signal attenuation at frequencies of 3, 10 e 30 kHz.

As expected, it was observed that this gain factor on resolution increases with the length of the FPC. This is explained by the fact that the fringe width decreases if the cavity length is increased, i.e, the channeled spectrum becomes denser. In our system, the DAQ board and tunable laser resolutions used in the quadrature-point tracker limits the useful cavity length to a maximum of 100 mm.

It is important notice that in some extent, it is feasible the tuning of the readout sensitivity by setting of some system design parameters. Indeed, the dynamic pressure sensitivity varies with the static pressure that is submitted to the sensing head. The magnitude of this variation depends on the mandrel dimensional parameters and the elastic properties of the mandrel material. The maximum static pressure that is supported by the sensor also depends of the dimensions and materials that were selected to the mandrel construction. In really, there is a trade off between the maximum static pressure and the sensor sensitivity. Another way to vary the

sensitivity is adjusting optical parameters, such as the interferometer path imbalance (in the case of interferometric based sensing heads) or the grating spectral width (when dealing with FBG based sensors). This flexibility is in the top of the basic feature of the interferometric optical sensing concept, which is its inherent high sensitivity.

This sensing head was immersed in oil to evaluate the sensor performance in a situation closer to the one present in a power transformer. To compare performances, results are also presented in the situations of the sensor in air (the reference selected) and in water, for an acoustic wave frequency of 20 kHz (Figure 10). The signal in liquid-immersed tests is stronger compared with the case of acoustic propagation in air, and a slower attenuation with distance is also observed.

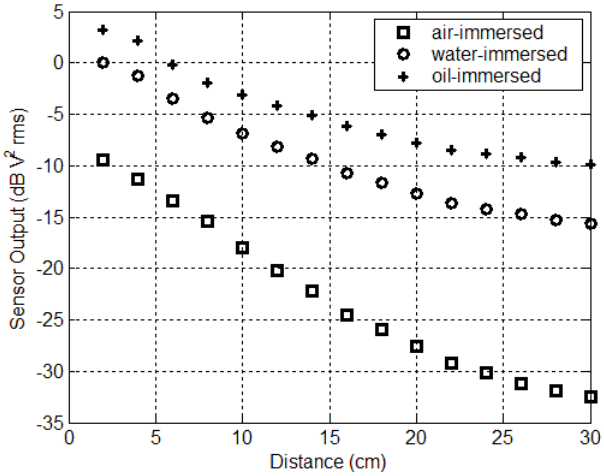

Fig. 10. Distance signal attenuation when the Fabry-Pérot sensing head is immersed in oil, water and air.

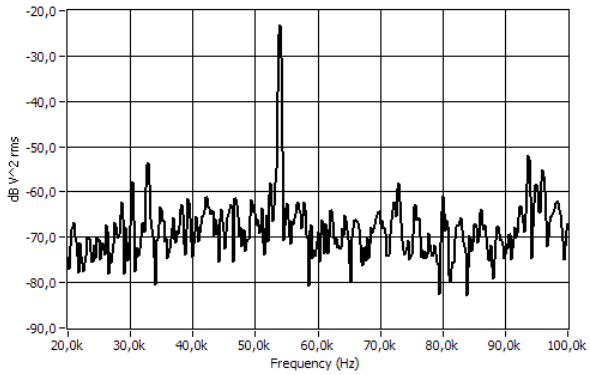

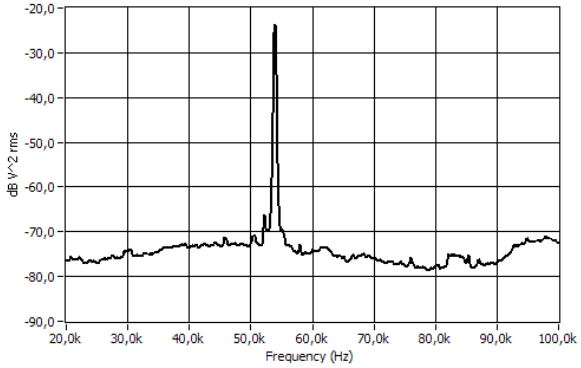

Fig. 11. Output signal of the FPI sensor with (up) air- and (down) oil-filled mandrel.

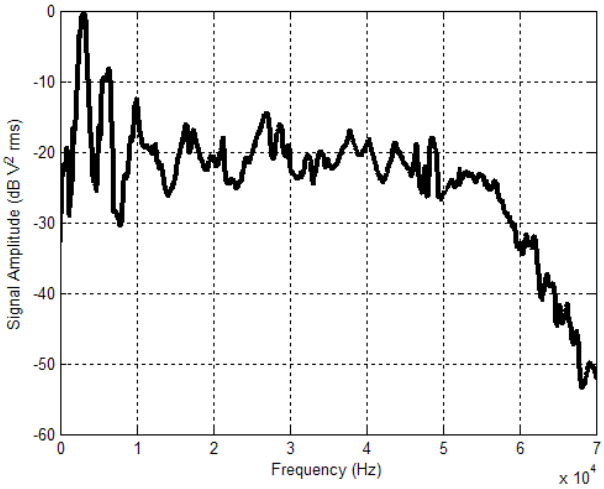

Fig. 12. Frequency response in water of the FPI sensing configuration.

Both features are positive, as well as the circumstance that for the case of propagation in oil at distances larger than 20 cm the attenuation does not increase substantially. This behavior is a consequence of the better acoustic energy transfer in a high density medium.

The effects caused by a change in the fluid inside the mandrel (air, water and oil) were also investigated. The obtained results indicate that when a viscous fluid is introduced in the cylinder, in spite of a possible slight decrease in peak signal amplitude, one important effect is observed: the improvement of the signal-to-noise ratio (Figure 11). These effects occur due to the mass effective addiction induced by the high density liquid inside the cylinder.

The sensor frequency response depends basically on the mandrel material (Young modulus and Poisson ratio) and its geometry (radius, length and thickness). The frequency spectrum was obtained experimentally using a signal generator to drive the PZT. Figure 12 shows this characteristic for the FPI sensor configuration when the frequency is swept from 1 to 70 kHz. The sweep function needs 1 min to cover the frequency range and the experiment was carried during 30 min. Thus, the data in the figure is a mean of 30 stored response values for each frequency. The first resonance appears at 3.3 kHz and the sensor response is relatively flat (ripple of ≈ 8 dB) in the range [10-50] kHz, but at higher frequencies the signal decreases dramatically (≈ 30 dB).

The first modal resonance frequency at 3.1 kHz was calculated by Eq. (1) and using the correction factor given by Eq. (5) to water-immersed tests, indicating a good agreement between the experimental data and the previsions derived from the mathematical vibration model.

V. Conclusion

This paper primary motivation was to demonstrate the feasibility of the application of new sensing concepts to acoustic detection of partial discharges. Globally, all results obtained are promising and globally consist of a *proof of concept*, confirming that partial discharge detection, optical transducing and measurement in power transformers is feasible using acoustic detection by sensor systems immersed in the oil, as an alternative to measurements taken from the exterior of the machine (using e.g. piezoelectric transducers).

Sensing head configurations based on a Michelson interferometer, a single FBG and a FBG based Fabry-Perot interferometer were investigated for the purpose of detecting the weak pressure wave from a partial discharge occurrence in power transformers. The three sensing structures were attached to the same compliant mandrel and all sensors were interrogated by an active homodyne scheme with a tunable laser, which is controlled by a computer-based feedback loop. The research developed allowed one to conclude that the FPI configuration with FBG reflectors is the one that shows the better performance in terms of pressure sensitivity.

The results are also pointing out that the proposed optical sensors, to be preferably mounted on the inside wall of the transformer tank (minimizing interference with the deployment of the electromagnetic field), present an enhanced sensitivity and superior performance for acoustic detection of PD activity when compared to the conventional piezoelectric sensors externally mounted. These characteristics of the intrinsic sensors approach are especially important to improve the PD location precision.

External mounted sensors have problems with signal attenuation and reflections on the tank wall. The sensing system proposed can overcome this issue and increase dramatically the accuracy of the acoustic PDs location; because it is able to detect directly the weak pressure disturbances produced by a PD activity and the acoustic signals can be separated from its reflections and the background noise by some methods of signal processing. Considering that the tank attenuation effect can be substantial, the possibility of inner tank placement of the optical sensors configures an intrinsic advantage of the proposed sensor system configuration if compared with the piezoelectric based ones. Other advantages of the proposed PD detection and location system include: the small size, high sensitivity, electrical nonconductivity and immunity to EMI.

Further work is in progress to move from prototype into industrial product, reaching a stage where the application of these sensors in power transformers becomes feasible. In particular, the effect of the mandrel geometry and material, the utilization of fibers of reduced diameter, and the feasibility of fiber laser sensing heads incorporating highly selective phase-shifted Bragg gratings are the object of study and optimization. Additionally, the process and the materials for sensing head fabrication are being appropriately selected to support some harsh conditions (e.g. corrosive environment, high temperature, high static pressure, etc.), aiming to improve the achievable readout resolutions as well as to flatten the frequency response of the optical fiber acoustic wave transducers. There are challenges to be faced to integrate a fiber sensing system into a power transformer, starting from the choice of the place inside the transformer where the sensors are to be deployed (windings, within the paper isolation, etc or preferably on the inner wall tank) to maximize acoustic capture and minimize electromagnetic field interference, which is theoretically expected to be minimal or negligible. Following this research, a new project is under development with a power transformers manufacturer to test these sensing heads into a real system with induced PD activity.

This development, which hopefully will lead to not too expensive technological solutions, opens also a new path for condition monitoring and incipient fault analysis: the placement of a number of sensors inside the transformer tank will allow the construction of 3-dimensional acoustic images that will allow the pinpointing of sources of noise and eventually lead to more accurate diagnosis.

References

[1] *IEEE Guide for the Detection and Location of Acoustic Emissions from Partial Discharges in Oil-Immersed Power Transformers and Reactors*, IEEE Standard C57.127-2007, Aug. 2007.

[2] L. Lundgaard, "Partial Discharge – Part XIV: acoustic partial discharge detection – practical application," *IEEE Electrical Insulation Magazine*, vol. 8, no. 5, pp. 34-43, 1992.

[3] P. Eleftherion, "Partial Discharge XXI: acoustic emission-based PD source location in transformers," *IEEE Electrical Insulation Magazine*, vol. 11, no. 6, pp. 22-26, 1995.

[4] R. Bartnikas, "Partial discharges. Their mechanism, detection and measurement," *IEEE Transactions on Dielectrics and Electrical Insulation*, vol. 9, no. 5, pp. 763-808, Oct. 2002.

[5] T. Bengtsson, B. Jönsson, "Transformer PD diagnosis using acoustic emission technique," in Proc. ISH-97, paper no. 115, 1997.

[6] J. H. Cole, R. L. Johnson, P. G. Bhuta, "Fiber-optic detection of sound," *J. Acoust. Soc. Amer.*, vol. 62, no. 5, pp. 1136-1138, Nov. 1977.

[7] J. A. Bucaro, T. R. Hickman, "Measurement of sensitivity of optical fibers for acoustic detection," *Appl. Opt.*, vol. 18, no. 6, pp. 938-940, 1979.

[8] R. O. Claus, J. H. Cantrell, "Detection of ultrasonic waves in solids by an optical fiber interferometer," in *Proc. 1980 Ultrasonics Symp.*, pp. 849-852, 1980.

[9] G. Wild, S. Hinckley, "Acousto-Ultrasonic Optical Fiber Sensors: Overview and State-of-the-Art," *IEEE Sensors Journal*, vol. 8, no. 7, pp. 1184-1193, 2008.

[10] J. A. Bucaro, H. D. Dardy, E. F. Carome, "Fiber-optic hydrophone," *J. Acoust. Soc. Amer.*, vol. 62, no. 5, pp. 1302-1304, Nov. 1977.

[11] J. Staudenraus, W. Eisenmenger, "Fibre-optic probe hydrophone for ultrasonic and shock-wave measurements in water," *Ultrasonics*, vol. 31, no. 4, pp. 267-273, Jul. 1993.

[12] G. A. Cranch, P. J. Nash, C. K. Kirkendall, "Large-scale remotely interrogated arrays of fiber-optic interferometric sensors for underwater acoustic applications," *IEEE Sensors Journal*, vol. 3, no. 1, pp. 19-30, Feb. 2003.

[13] J. M. Lopez-Higuera, *Handbook of Optical Fiber Sensing Technology*, Wiley, New York, 2002.
[14] S. Atique, D. Betz, B. Culshaw, F. Dong, H. S. Park, G. Thursby, B. Sorazu, "Detecting ultrasound using optical fibres," *J. Optics*, vol. 33, no. 4, pp 231-238, 2004.
[15] W. Lin, C. F. Chang, C. W. Wu, M. C. Chen, "The configuration analysis of fiber optic interferometer of hydrophones," in Proc. Oceans '04 MTS/IEEE Techno-Ocean '04 (IEEE Cat. No.04CH37600), IEEE, vol. 2, pp. 589-592, 2004.
[16] E. Udd, "Fiber-optic acoustic sensor based on the Sagnac interferometer," *Proc. SPIE*, vol. 425, pp. 90-95, 1983.
[17] D. J. Webb, J. Surowiec, M. Sweeney, D. A. Jackson, J. M. Hand, L. Gavrilow, L. Zhang, I. Bennion, "Miniature fiber optic ultrasonic probe," *Proc. SPIE*, vol. 2839, pp. 76-80, 1996.
[18] N. Takahashi, K. Yoshimura, S. Takahashi, K. Imamura, "Development of an optical fiber hydrophone with fiber Bragg grating," *Ultrasonics*, vol. 38, pp. 581-585, no. 1-8, Mar. 2000.
[19] M. Leblanc, C. Kirkendall, A. Dandridge, "Acoustic sensing using free and transducer-mounted fiber Bragg gratings," in *Proc. OFS-14*, pp. 592–595, 2000.
[20] I. Perez, H. L. Cui, E. Udd, "Acoustic emission detection using fiber Bragg gratings," in *Proc. SPIE - Smart Structures and Materials*, vol. 4328, pp. 209-215, 2001.
[21] D. C. Betz, G. Thursby, B. Culshaw, W. J. Staszewski, "Acousto-ultrasonic sensing using fiber Bragg gratings," *Smart Materials and Structures*, vol. 12, no. 1, pp. 122-128, Feb. 2003.
[22] A. Minardo, A. Cusano, R. Bernini, L. Zeni, M. Giordano, "Response of fiber Bragg gratings to longitudinal ultrasonic waves," *IEEE Trans. Ultras. Ferroelec. Freq. Contr.,* vol. 52, no. 2, pp. 304-312, Feb. 2005.
[23] T. Fujisue, K. Nakamura, S. Ueha, "Demodulation of acoustic signals in fiber Bragg grating ultrasonic sensors using arrayed waveguide gratings," *J. J. Appl. Phys.*, vol. 45, no. 5B, pp. 4577-4579, May 2006.
[24] V. Miranda , A.R.G. Castro, "Improving the IEC table for transformer failure diagnosis with knowledge extraction from neural networks," *IEEE Trans. on Power Delivery*, vol. 20, no. 4, pp. 2509-2516, Oct. 2005.
[25] S. N. Hettiwatte, Z. D. Wang, P. A. Crossley, "Investigation of propagation of partial discharges in power transformers and techniques for locating the discharge," *IEE Proceedings Science, Measurement and Technology*, vol. 152, no. 1, pp. 25-30, 2005.
[26] A. Zargari, T. R. Blackburn, "Application of optical fiber sensor for partial discharge detection in high-voltage power equipment," *IEEE Annual Report – Conference on Electrical Insulation and Dielectric Phenomena*, pp. 541-544, 1996.
[27] A. Zargari, T. R. Blackburn, "Acoustic detection of partial discharges using non-intrusive optical fiber sensors," in *Proc. IEEE International Conference on Conduction and Breakdown in Solid Dielectrics*, pp. 573-576, 1998.
[28] Z. Zhao, "Fiber optic acoustic sensing and locating of partial discharges in high-voltage oil-filled power transformers," PhD Dissertation: The Hong Kong Polytechnic University, 1998.
[29] B. Yu, D. W. Kim, J. Deng, H. Xiao, A. Wang, "Fiber Fabry-Perot sensors for detection of partial discharges in power transformers," *Applied Optics*, vol. 42, no. 16, pp. 3241-3250, 2003.
[30] N. Zeng, C. Shi, D. Wang, M. Zhang, Y. Liao, "Diaphragm-type fiber-optic interferometric acoustic sensor," *Opt. Eng.*, vol. 42, no. 9, pp. 2558-2562, 2003.
[31] J. Xu, X. Wang, K. Cooper, A. Wang, "Miniature all-silica fiber optic pressure and acoustic sensors," *Opt. Lett.*, vol. 30, no. 24, pp. 3269-3271, 2005.
[32] T. Bengtsson, M. Leijon, L. Ming, "Acoustic frequencies emitted by partial discharges in oil," in *Proc. ISH-93*, paper no. 63.10, 1993.
[33] T. Krauthammer and E. Ventsel, Thin *Plates and Shells: Theory, Analysis and Applications*, 1st ed., Mercel Dekker Inc., New York, 2001, pp. 609 – 618.
[34] W. Soedel, *Vibrations of Shells and Plates*, 3rd ed., Mercel Dekker Inc., New York, 2004, pp. 93-101.
[35] M. Anghinolfi, A. Calvi, A. Cotrufo, M. Ivaldi, O. Yershova, F. Parodi, D. Piombo, A. Plotnikov and L. Repetto, "A Fiber Optic Air Backed Mandrel Hydrophone to Detect High Energy Hadronic Showers in the Water," in Workshop of the Russian-Italian collaboration in the Cosmic Ray Physics, Moscow, pp. 1–9, 2005.

Sanderson E.U. Lima (S'08) received his graduation and MSc degrees in electrical engineering from the Federal University of Ceará (UFC), Brazil, in 2003 and 2005, respectively, and is a PhD student at the University of Porto with a fellowship of AlBan Programme (E05D054697BR). He is a researcher with INESC Porto. His interests are power system equipment diagnosis and optical sensing applications.

Orlando Frazão graduated in physics engineering (optoelectronics and electronics) from the University of Aveiro. From 1997 to 1998 he was with the Institute of Telecommunications, Aveiro. He is currently a development senior engineer with INESC Porto. His research interests include applications of Bragg grating technology in optical sensors and optical communications.

Rubem G. Farias graduated in 1974 in electrical engineering from the Federal University of Pará (UFPA), received his MSc degree in electronic engineering in Technological Institute of Aeronautics (ITA) in 1983 and received PhD degree in electrical engineering from the State Univerty of Campinas (Unicamp) in 1996. Dr. Farias is a Professor Titular (Full Professor) in Federal University of Pará (UFPA). He is currently a post-doctoral research fellow with INESC Porto, Portugal.

Francisco M. Araújo graduated in 1993 in applied physics (optics and electronics) from the University of Porto, Portugal, where he received his PhD degree in physics in 2000. He is a senior researcher with INESC Porto. His main activity involves optical communications and fiber optic sensing. He is also a cofounder of FiberSensing, an INESC Porto spin-off company developing fiber optic sensors and monitoring systems.

Luís A. Ferreira graduated in applied physics (optics and electronics) in 1991 and received his MSc degree in optoelectronics and lasers in 1995, both from the University of Porto, Portugal, where he received his PhD degree in physics in 2000. He is a senior researcher with INESC Porto. His main activity involves optical communications and fiber optic sensing. He is also a cofounder of FiberSensing, an INESC Porto spin-off company developing fiber optic sensors and monitoring systems.

José L. Santos graduated in 1983 in applied physics (optics and electronics) from the University of Porto, Portugal, where he received his PhD degree in physics in 1993 for research on fiber optic sensing. He is an associate professor in the Physics Department of the University of Porto and is in charge of the Optoelectronics and Electronic Systems Unit of INESC Porto. His main research interest is optical fiber sensing. He is a member of OSA and SPIE.

Vladimiro Miranda (M'90-SM'04-F'05) received his graduation, Ph.D. and Agregado degrees from the Faculty of Engineering of the University of Porto, Portugal (FEUP) in 1977, 1982 and 1991, all in Electrical Engineering. In 1981 he joined FEUP and currently holds the position of Professor Catedrático (Full Professor). He is also a researcher at INESC since 1985 and is currently Director of INESC Porto, an advanced research institute in Portugal. He has authored many papers and been responsible for many projects in areas related with the application of Computational Intelligence to Power Systems.